# 5.2 THE EFFECT OF TURBULENCE ON CLOUD MICROSTRUCTURE, PRECIPITATION FORMATION AND THE ORGANISATION OF STRATOCUMULUS AND SHALLOW CUMULUS CONVECTION

Charmaine N. Franklin *
Centre for Australian Weather and Climate Research
A partnership between CSIRO and the Australian Bureau of Meteorology, Aspendale, Victoria, Australia

## 1. INTRODUCTION

The effect of aerosols on clouds remains one of the largest sources of uncertainty in climate studies and many of the complex aerosol-cloud interactions are associated with cloud microphysical processes. To enable greater confidence in climate projections one of the processes that requires a quantitative analysis is the second indirect aerosol effect, which is the effect from enhanced aerosol concentrations in clouds suppressing drizzle and prolonging cloud lifetimes (Albrecht 1989). To be able to quantify this effect with any real certainty, the cloud microphysical processes must be accurately represented in global climate models (GCMs), in particular the autoconversion process, which describes the collision and coalescence of small cloud droplets to form larger raindrops. Rotstayn and Liu (2005) demonstrated how changing autoconversion schemes in a GCM could decrease the globally averaged second indirect aerosol effect by 60%, highlighting the need for increased understanding and a more accurate parameterization of autoconversion.

In clouds where the temperature does not reach freezing, it is the process of collision and coalescence that allows drops to grow to a size large enough to fall out of a cloud as rain. Observations of droplet growth tend to show a faster evolution and broader drop size distribution compared to the theoretically calculated drop spectra, where the equations are applied to a randomly distributed population of drops whose motion is governed by gravitational forcing. Several physical effects have been suggested to play an important role in the reduction of the growth times, including entrainment and mixing of dry air, turbulence and the role of giant cloud condensation nuclei (e.g. Beard and Ochs 1993). Turbulence increases the collision rate of droplets in at least three ways: by changing the droplet velocities and the spatial distribution of the droplets (e.g. Franklin et al. 2005), and by changing the collision and coalescence efficiencies between droplets. Although the effect of turbulence on cloud droplet collision-coalescence rates is yet to be quantified by observations, recent modeling studies have shown that turbulence can increase the collision rates of droplets by several times the purely gravitational rate (Franklin et al. 2005, 2007; Wang et al. 2005; Pinsky et al. 2006).

Franklin et al. (2007) performed direct numerical simulations (DNS) of droplets within turbulent flow fields and developed empirically derived equations that describe the turbulent collision kernel for droplet pairs, where the larger droplet is within the radius range of 10 – 30 μm and the eddy dissipation rate of turbulent kinetic energy (TKE) is between 100 and 1500 $cm^2$ $s^{-3}$. These turbulent collision kernels were used in solutions of the stochastic collection equation (SCE) by Franklin (2008) to develop model-based empirical double-moment parameterizations of the effect of autoconversion, accretion and self-collection on the rain and cloud water mixing ratios and the rain and cloud drop number concentrations. Parameterizations using both turbulent and non-turbulent collision kernels were developed. The SCE was solved for liquid water contents in the range of 0.01 – 2 g $kg^{-1}$, cloud droplet number concentrations up to 500 drops $cm^{-3}$ and relative dispersion coefficients of the initial drop size distribution between 0.25 and 0.4. The initial drop size distribution was a Gamma function and the separation radius that determined the point at which a cloud droplet becomes a raindrop was 40 μm. Using the SCE results for such a broad range of drop size distributions gives the resulting parameterizations greater statistical meaning and applicability. The two suites of warm rain parameterizations, turbulent and non-turbulent, allow the investigation of the effect of turbulence on the microphysical processes and the resulting feedbacks in atmospheric models. These effects are explored in this work for stratocumulus and shallow cumulus convection cases.

## 2. EXPERIMENT DESIGN

The double-moment warm rain microphysics parameterizations of Franklin (2008) have been implemented in the UCLA large eddy simulation (LES) model. The turbulent autoconversion equation has been modified to the following form, which gives a better representation of the DNS data at higher cloud water contents

$$\frac{\partial q_r}{\partial t}\Big|_{auto} = 2.0026\times10^{3}\tan\left(-5.2\times10^{-2}R_\lambda + 15.78\right)$$

$$q_c^{\,97.45\left(-8.4\times10^{-1}\right)^{R_\lambda}+2.5}\; N_c^{\,1\Big/\left(-9.0\times10^{-1}+1.28\times10^{-2}R_\lambda-2.3\times10^{-4}R_\lambda^{\,2}\right)}$$

where $q_r$ and $q_c$ are the rain and cloud water contents (kg $m^{-3}$), $N_c$ is the cloud droplet concentration ($cm^{-3}$) and $R_\lambda$ is the Taylor microscale Reynolds number of the flow field (see Franklin 2008 for information on relevant Reynolds numbers for DNS). The LES code is described in detail in Stevens et al. (2005) and solves prognostic equations for the three velocity components,

*Corresponding author address:
Charmaine N. Franklin, CSIRO Marine and Atmospheric Research, Private Bag No. 1, Aspendale, Victoria, 3195, Australia; E-mail: charmaine.franklin@csiro.au

the total water mixing ratio, the liquid water equivalent potential temperature and the mass and number concentration of rain. The mass of cloud water is defined implicitly due to the dependence of the liquid water potential temperature on the total condensate, and the cloud droplet number concentration is a fixed parameter. The numerical solution of the cloud processes, including droplet sedimentation, is described in Savic-Jovcic and Stevens (2008).

### 2.1 Description of the Shallow Cumulus Convection Case - RICO

The domain size of these experiments is 13.2 km square and 5 km deep, with grid spacing of 100 m in the horizontal and 40 m in the vertical. The time step is variable and is chosen as to keep the Courant number between 0.65 and 0.85. The initial and boundary conditions and large scale forcings are taken from the GEWEX Cloud Systems Study (GCSS) intercomparison case (http://www.knmi.nl/samenw/rico/). The average observed cloud droplet number concentration during RICO was 70 $cm^{-3}$, and that number has been used for the control simulations. The length of the simulations for this case are 24 hours and the profile statistics are taken as averages over the last 4 hours. After the initial spin up, the model produces numerous shallow precipitating convective clouds as shown in Figure 1a. The clouds typically extend up to 2400 m, have cloud bases at around 600 m and tend to be 1-2 km in horizontal extent (see Fig. 2b).

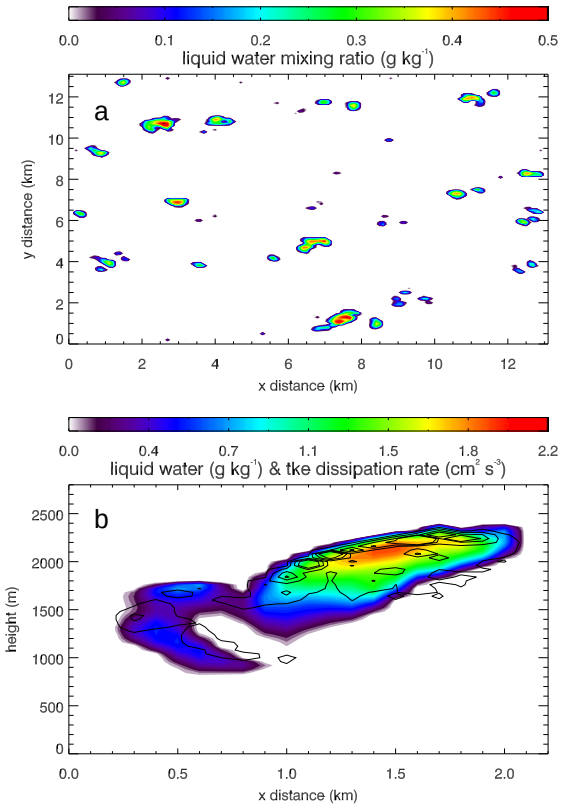


Figure 1. a) Plan view of RICO liquid water at 840 m and b) cross-section through a typical cloud showing liquid water and contour lines of the dissipation rate of TKE (contour levels are 100, 500, 1000, 1500 $cm^2$ $s^{-3}$).

### 2.2 Description of the Stratocumulus Case – DYCOMS II

The horizontal domain and grid spacing for this case study are 6.6 km and 50 m respectively, while the vertical domain is 2 km and the grid spacing varies from 5 m at the surface and the inversion to 80 m at the model top. The large-scale forcings are taken form the GCSS intercomparison study documented in Ackerman et al. (2009). The control case uses the observed average cloud droplet number concentration of 55 $cm^{-3}$. The model is run for 6 hours and the profile statistics are calculated over the final 4 hours. This case consists of a nocturnal stratocumulus under a dry inversion with embedded pockets of heavy drizzling open cellular convection. Typical liquid and rain water cross sections are shown in Figure 2.

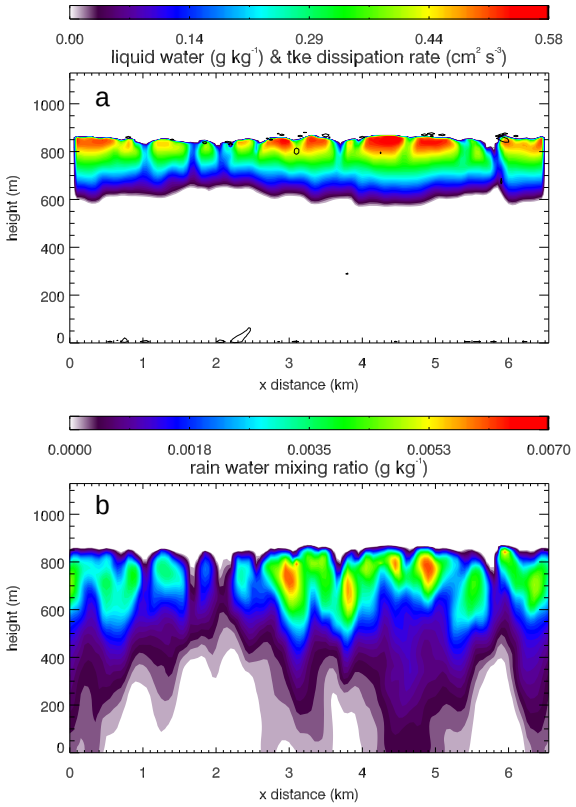


Figure 2. Cross sections of the liquid and rain water for the DYCOMS II case. Contour lines of the TKE dissipation rate are 10 and 100 $cm^2$ $s^{-3}$.

## 3. RESULTS

### 3.1 Shallow Cumulus Convection - RICO

The turbulent microphysics parameterizations are applied in the regions of the clouds where the dissipation rates of TKE are between 100 and 1500 $cm^2$

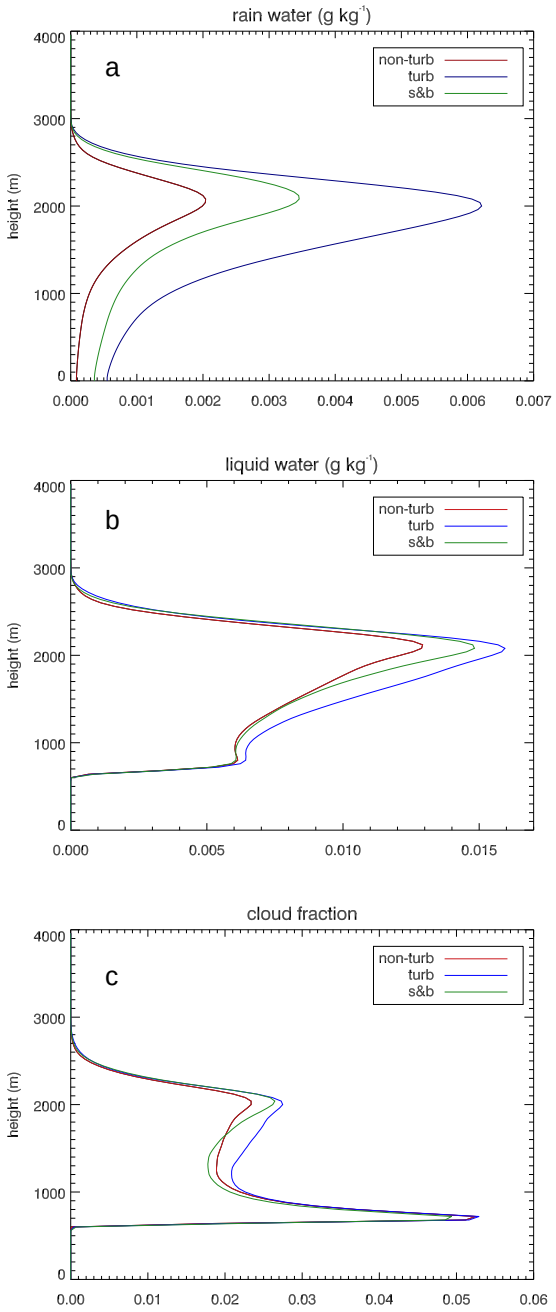


Figure 3. RICO cloud properties for the simulations that use the turbulent and non-turbulent microphysics parameterizations of Franklin (2008) and the microphysics scheme of Seifert and Beheng (2001).

$s^{-3}$, with the higher dissipation rates associated with faster conversion rates from cloud to rain water (see Franklin 2008). In the RICO case the range of dissipation rates for which the turbulent microphysics scheme is valid is encountered in extensive regions of the clouds, with the highest dissipation rates occurring near the cloud tops (see Fig. 1b). These increased autoconversion, accretion and self-collection rates increase the rain water mixing ratio of the clouds as compared to the simulation where the non-turbulent parameterization is used as shown in Figure 3a. The results using the well known Seifert and Beheng (2001) (SB) scheme are included as a measure of confidence for the new schemes of Franklin (2008), however, due to the very different nature of the schemes a comparison is beyond the scope of this paper and rather the focus is on the differences between the turbulent and non-turbulent results.

Even though the rain water contents are significantly increased when the turbulent microphysics effects are included, the cloud fractions do not differ much. The largest difference in cloud fraction occurs in the levels above 1000 m, where more cloud water in the turbulent case generates greater cloud fractions (see Figures 3b and c). The simulation using the turbulent microphysics parameterization has on average greater cloud water throughout the cloud, however, the percentage increase in the amount of rain water produced in this simulation compared to the case using the non-turbulent microphysics is far more than the increase in the cloud liquid water contents. When the cloud droplet number concentration (CDNC) is reduced, the precipitation rates are increased for all schemes. Reducing the droplet number concentration in the non-turbulent microphysics case from 70 drops $cm^{-3}$ to 40 $cm^{-3}$ produces an average rainwater amount that is still less than that of the turbulent microphysics control case (not shown). The peak rainwater amount at 2000 m in the non-turbulent case with 40 drops $cm^{-3}$ is about 60% of the turbulent microphysics result with 70 drops $cm^{-3}$.

Figure 4a shows that the evaporation of rain water is greatly enhanced in the turbulent microphysics simulation due to an increase in both rain water and rain drop number. The average vertically integrated TKE from the simulation using the turbulent microphysics is less than that of the non-turbulent case in the upper cloud levels above 2000m (see Fig. 4b), however, in the lower levels, particularly below cloud base, the TKE from the turbulent case is greater than the non-turbulent case. The increased TKE in the subcloud layer of the turbulence runs reflects the greater horizontal variability associated with the enhanced evaporation of precipitation destabilizing the levels below the cloud, as shown in Figure 4c. In the turbulent microphysics simulation the reduced TKE in the upper regions of the cloud is caused by the increased latent heating associated with the increased cloud and rain water in this case. This increase in the latent heating compared to the non-turbulent microphysics simulation reduces the entrainment and the buoyancy production of TKE (see Fig. 4d). The reduced buoyancy and entrainment in the upper levels of the cloud in the turbulent case cause a reduction in the variance of the vertical motion as shown in Figure 4d. The updrafts within the clouds in the turbulent case are stronger in the upper levels due to the increased latent heating associated with the larger generation of rain and cloud liquid water.

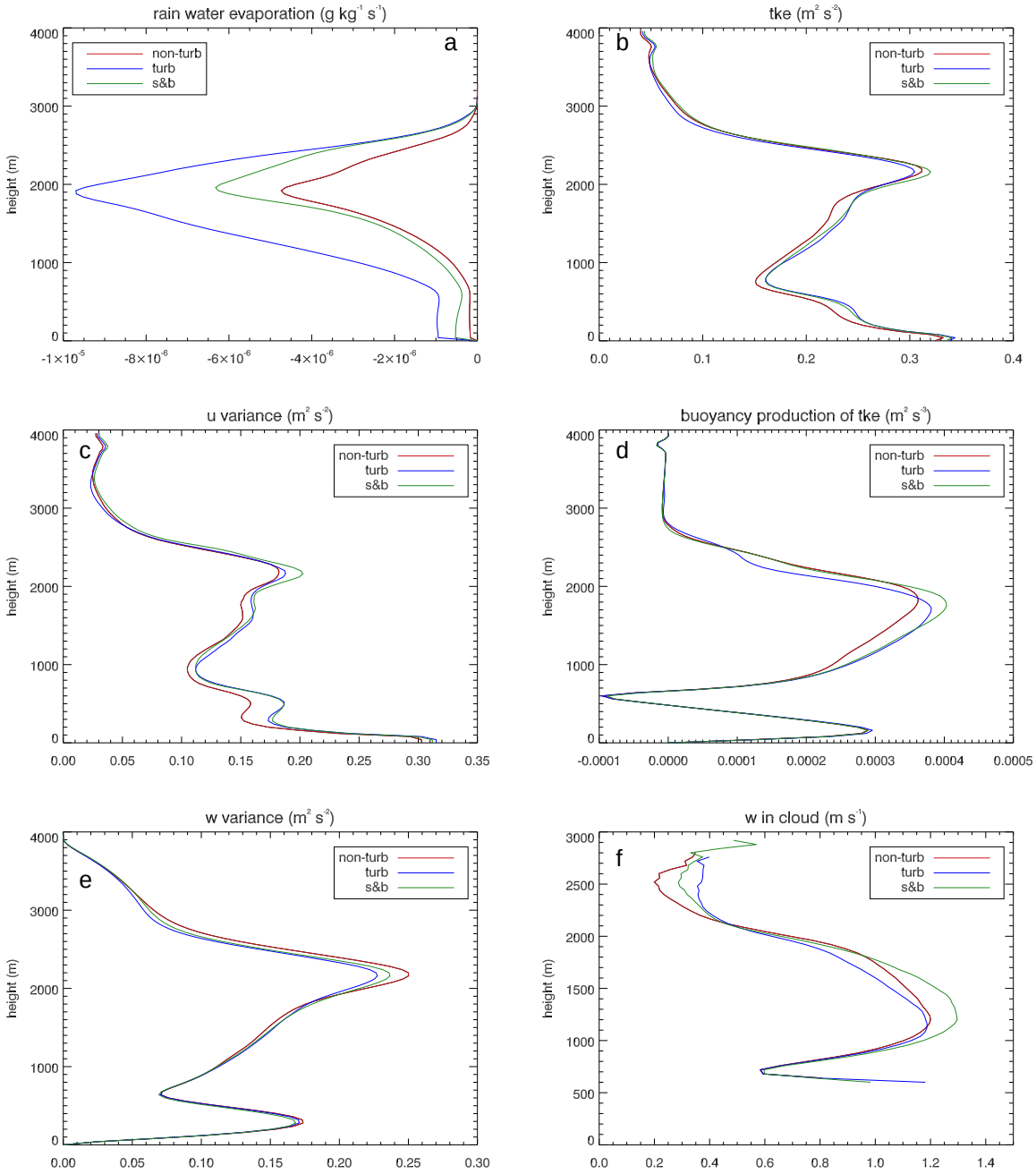


Figure 4. RICO cloud and dynamical properties for the simulations that use the turbulent and non-turbulent microphysics parameterisations of Franklin (2008) and Seifert and Beheng (2001).

### 3.2 Stratocumulus – DYCOMS II

Similar to the shallow convection case, the dissipation rates of TKE are maximal in the upper levels of the stratocumulus cloud layer, however, for this case the dissipation rates are much weaker. There are only small regions at the top of the cloud where the dissipation rate reaches 100 $cm^2$ $s^{-3}$ (see Fig. 3b) and, therefore, where the conversion rates between cloud and rain water will be accelerated by turbulence effects. These small regions though do make a difference to the precipitation flux both in the cloud layer and the subcloud layer as shown in Figure 5a, while the cloud fractions remain unchanged (see Fig. 5b). For this case the microphysics scheme of Khairoutdinov and Kogan (2000) has been used as a comparison for the new schemes, however, the results from the K&K scheme will not be discussed in this paper as the focus is on the turbulence effects.

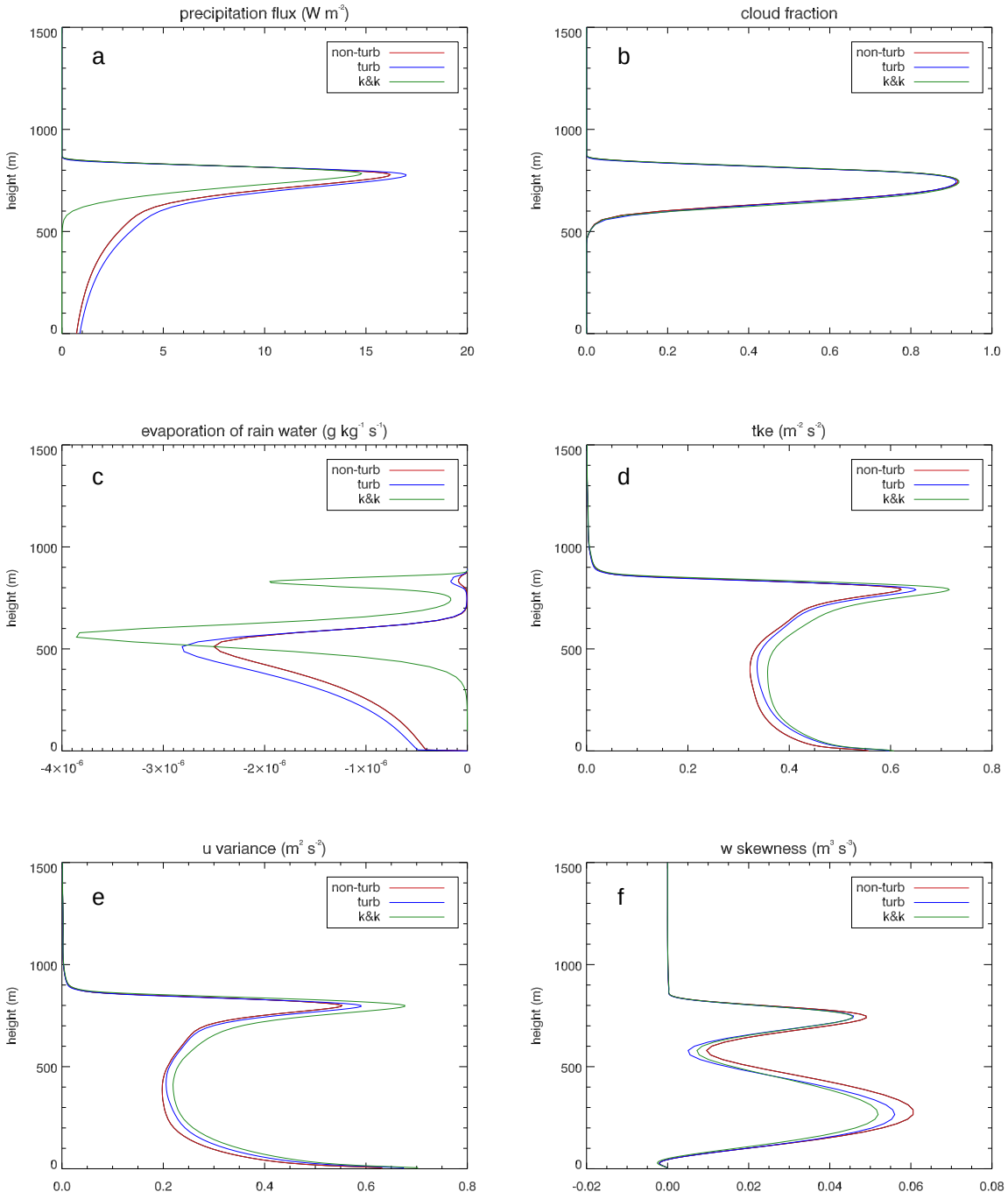


Figure 5. DYCOMS II cloud and dynamical properties for the simulations that use the turbulent and non-turbulent microphysics parameterisations of Franklin (2008) and the microphysics scheme of Khairoutdinov and Kogan (2000).

The increased rain water in the turbulent microphysics simulation is associated with a greater number of rain drops and larger evaporation rates of rain water, particularly at cloud base (see Figure 5c). As for the shallow convection case, the increased evaporation leads to greater variability and higher TKE in the turbulent simulation as shown in Figures 5d and e. In this case the stronger circulations occur both in the subcloud layer and at the top of the cloud layer. The enhanced rain water in the turbulent microphysics simulation has a positive feedback in this case, with more rain producing more evaporation of drizzle drops at cloud base, which destabilizes the subcloud layer and leads to stronger circulations and TKE. The observations for this case showed that the vertical winds were negatively skewed just above

cloud base (Ackerman et al. 2009) and the simulation with the turbulent microphysics produces a closer match with nearly equal strength between updrafts and downdrafts at this height (see Fig. 5f).

## 4. AEROSOL EFFECTS - AVERAGED CLOUD PROPERTIES AT DIFFERENT CLOUD DROPLET CONCENTRATIONS

Four simulations of the stratocumulus case were performed with each of the non-turbulent and turbulent microphysics parameterizations. The simulations differ in the prescribed CDNC and reveal how the cloud properties change with changes in aerosol loading as manifested in changes of cloud droplet number. Figure 6 shows the average cloud properties over the last 4 hours of the DYCOMS II simulations. The cloud fraction increases monotonically for both the non-turbulent and turbulent cases as the CDNC is increased (see Fig. 6a). There is a strong relationship between increasing cloud fraction and decreasing rain water path as the CDNC is increased. This result for a stratocumulus cloud agrees with the conceptual model that greater aerosol loading suppresses precipitation formation and leads to larger cloud fractions. For the CDNC values explored herein the non-turbulent microphysics simulations demonstrate that stratocumulus clouds typical of this case study increase the amount of cloud water and reduce the rain water content when there is an increase in cloud droplet number, therefore, they show a positive second aerosol indirect effect (Fig. 6b). While this is also true for the lowest three CDNC used in this study for the turbulent microphysics, for the maximum concentration of 200 drops $cm^{-3}$ the turbulent simulation shows a reduction in both the rain and liquid water paths. Other studies have also shown a non-monotonic increase in LWP with increasing aerosol concentrations and suggest that there is a limit to the degree of liquid water that can build up in stratocumulus clouds. The reduced rain water leading to a reduced liquid water path in the turbulent simulation with highest CDNC shows a negative second aerosol indirect effect.

Figure 6c shows that there is an increase in the cloud base heights as cloud droplet numbers are increased and precipitation is decreased. The cloud base lowers in regions of precipitation due to the precipitation changes affecting the thermodynamic state of the subcloud layer. This is also shown by the lower and more variable cloud fractions of the turbulence simulations, suggesting that the evaporation of the enhanced precipitation plays an important role in reorganizing the circulations. The TKE increases with CDNC in all simulations except for the turbulent case with highest CDNC as shown in Figure 6d.

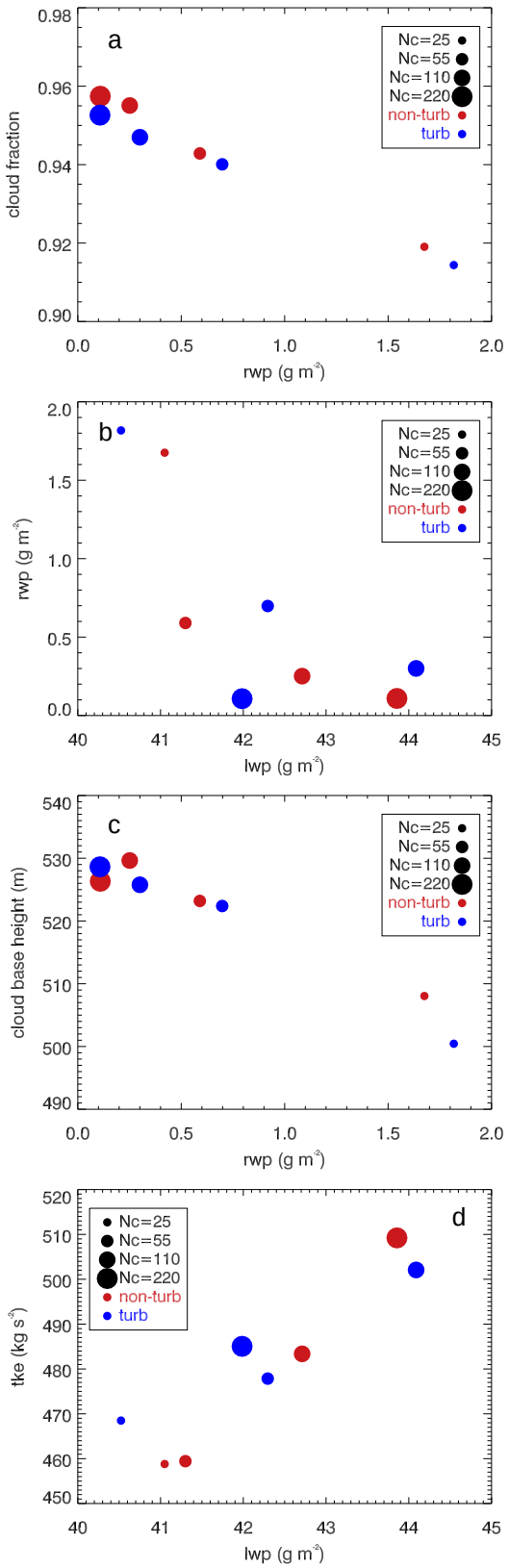


Figure 6. Average DYCOMS II cloud and dynamical properties for specified CDNC.

Figure 7 shows the effects of increasing the CDNC in the RICO simulations. In these shallow cumulus convection cases the liquid water path increases as the rain water path increases (see Fig 7a), which is the opposite of the stratocumulus case of DYCOMS II. Increased CDNC results in reduced rainwater in both cases, but in the RICO cases this also results in reduced liquid water paths. The increased CDNC will tend to slow the collision-coalescence process, enhance evaporation and reduce the drop fall speeds. The result of this and the subsequent feedbacks in these small clouds is to reduce the liquid water path as well as the amount of precipitation. All cases, therefore, simulate a negative second aerosol indirect effect except for the highest CDNC using the non-turbulent microphysics scheme, which shows a small increase in liquid water path. The change in average cloud fraction for all simulations is small and generally less than 1%.

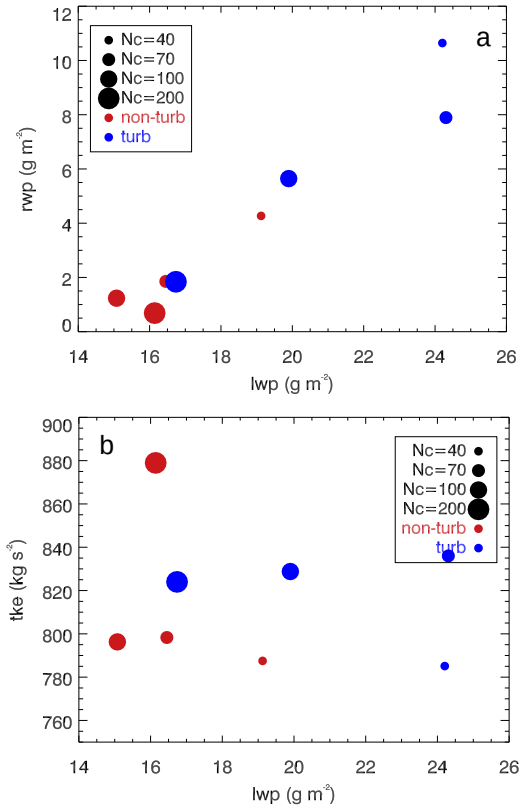


Figure 7. Average RICO cloud and dynamical properties for specified CDNC.

The TKE response to increased CDNC is shown in Figure 7b. The non-turbulent microphysics simulations tend to show an increase in vertically averaged TKE as CDNC increases, while the turbulent microphysics cases show a decrease in TKE for the three higher CDNC cases. The reduction in TKE and rain water for the turbulent microphysics cases may be due to the negative feedback that the enhanced precipitation has on the entrainment and buoyancy production of TKE as discussed previously.

## 5. CONCLUSIONS

The use of new warm rain microphysics parameterizations has allowed an investigation into the effects of turbulence on cloud microphysical processes in stratocumulus and shallow convective clouds. Turbulence had a greater effect on the simulated precipitation rates in the shallow convection case where the larger TKE dissipation rates produced a more rapid conversion of cloud water to rain water. The much weaker dissipation rates in the stratocumulus case, however, also showed a change in the simulated precipitation when the effects of turbulence on microphysical processes were included in the LES model. Both cases using the turbulent microphysics scheme produced greater evaporation rates of rain water, which caused a change in the thermodynamics of the subcloud layer, destabilizing the lower levels and enhancing the horizontal variability and TKE in this region. The difference between the two cases in the effect of the turbulent microphysics was at the upper levels of the clouds. In the shallow convection case the enhanced latent heating associated with the greater rain and cloud liquid water reduced the entrainment and buoyancy production of TKE, therefore, producing a negative feedback to the enhanced precipitation formation associated with turbulent effects. In contrast, the stratocumulus case showed a positive feedback with enhanced rainwater producing greater TKE in both the subcloud layer and in the upper cloud region. Including the effects of turbulence in the microphysics parameterizations minimizes the need to artificially reduce CDNC in order to simulate observed precipitation rates.

Sensitivity studies where the CDNC was varied showed agreement with the conceptual model for lightly drizzling stratocumulus clouds that greater aerosol loading, as manifested in greater CDNC, suppresses precipitation formation leading to larger cloud fractions and liquid water paths. This positive second indirect aerosol effect was produced in all of the DYCOMS II simulations except for the case using the turbulent microphysics with the highest CDNC, which showed that there may be a limit to the amount of liquid water that can build up in this stratocumulus case. The shallow convection case of RICO produced a negative second indirect aerosol effect in all but one simulation. The increased CDNC in the small convective clouds reduced the production of rainwater, enhanced the evaporation and led to a reduction in the liquid water path.


## Acknowledgements

This work was supported by the Australian Department of Climate Change. Bjorn Stevens from the Max Planck Institute for Meteorology and Verica Savic-Jovcic from UCLA are thanked for providing the

UCLA LES model code and the settings for the RICO and DYCOMS II experiments.

**References**


Ackerman, A.S., and coauthors, 2009: Large-eddy simulations of a drizzling, stratocumulus-topped marine boundary layer. *Mon. Wea. Rev.,* 137, 1083-1110.

Albrecht, B.A., 1989: Aerosols, cloud microphysics, and fractional cloudiness. *Science*, 245, 1227-1230.

Beard, K.V. and H.T. Ochs, 1993: Warm-rain initiation: An overview of microphysical mechanisms. *J. Appl. Meteor.,* 32, 608-625.

Franklin, C.N., P.A. Vaillancourt, M.K. Yau, and P. Bartello, 2005: Collision rates of cloud droplets in turbulent flow. *J. Atmos. Sci.,* 62, 2451-2466.

Franklin, C.N., P.A. Vaillancourt, and M.K. Yau, 2007: Statistics and parameterizations of the effect of turbulence on the geometric collision kernel of cloud droplets. *J. Atmos. Sci.,* 64**,** 938-945.

Franklin, C.N., 2008: A warm rain microphysics parameterization that includes the effects of turbulence. *J. Atmos. Sci.,* 65, 1795-1816.

Khairoutdinov, M. and Y. Kogan, 2000: A new cloud physics parameterization in a large-eddy simulation model of marine stratocumulus. *J. Atmos. Sci.,* 57, 229-243.

Pinsky, M.B., A.P. Khain, B. Grits and M. Shapiro, 2006: Collisions of small drops in a turbulent flow. Part III: Relative droplet fluxes and swept volumes. *J. Atmos. Sci.,* 63, 2123-2139.

Rotstayn, L.D., and Y. Liu, 2005: A smaller global estimate of the second indirect aerosol effect. *Geophys. Res. Lett.,* 32, L05708, doi:10.1029/2004GL021922.

Saviv-Jovcic, V. and B. Stevens, 2008: The structure and organization of precipitating stratocumulus. *J. Atmos. Sci.,* 65, 1587-1605.

Seifert, A., and K.D. Beheng, 2001: A double-moment parameterization for simulating autoconversion, accretion and selfcollection. *Atmos. Res.,* 59-60, 265-281.

Stevens, B., and coauthors, 2005: Evaluation of large-eddy simulations via observations of nocturnal marine stratocumulus. *Mon. Wea. Rev.,* 133, 1443-1462.

Wang, L.-P., O. Ayala, S.E. Kasprzak and W.W. Grabowski, 2005: Theoretical formulation of collision rate and collision efficiency of hydrodynamically interacting cloud droplets in turbulent atmosphere. *J. Atmos. Sci.,* 62, 2433-2450.